

Exposure to heavy metal-contaminated sediments disrupts gene expression, lipid profile, and life history traits in the midge *Chironomus riparius*

Hélène Arambourou ^{a,1}, Lola Llorente ^{b,1}, Iñigo Moreno-Ocio ^c, Óscar Herrero ^b, Carlos Barata ^d, Inmaculada Fuertes ^d, Nicolas Delorme ^a, Leire Méndez-Fernández ^e, Rosario Planelló ^{b,*}

^a IRSTEA Lyon, Riverly Research Unit, Villeurbanne, France

^b Biology and Environmental Toxicology Group, Faculty of Science, Universidad Nacional de Educación a Distancia (UNED), Madrid, Spain

^c Department of Zoology and Animal Cellular Biology, University of the Basque Country (UPV/EHU), Leioa, Spain

^d Department of Environmental Chemistry, Institute of Environmental Assessment and Water Research (IDAEA), Spanish Research Council (CSIC), Barcelona, Spain

^e Department of Plant Biology and Ecology, University of the Basque Country (UPV/EHU), Leioa, Spain

ARTICLE INFO

Article history:

Received 17 April 2019

Received in revised form

28 September 2019

Accepted 5 October 2019

Available online 7 October 2019

Keywords:

Larval development

Lipidomic

Transcriptional alterations

Shape markers

Integrative approach

Endocrine disruption

ABSTRACT

Despite the concern about anthropogenic heavy metal accumulation, there remain few multi-level ecotoxicological studies to evaluate their effects in fluvial ecosystems. The toxicity of field-collected sediments exhibiting a gradient of heavy metal contamination (Cd, Pb, and Zn) was assessed in *Chironomus riparius*. For this purpose, larvae were exposed throughout their entire life cycle to these sediments, and toxic effects were measured at different levels of biological organization, from the molecular (lipidomic analysis and transcriptional profile) to the whole organism response (respiration rate, shape markers, and emergence rate). Alterations in the activity of relevant genes, as well as an increase of storage lipids and decrease in membrane fluidity, were detected in larvae exposed to the most contaminated sediments. Moreover, reduced larval and adult mass, decrease of larval respiration rate, and delayed emergence were observed, along with increased mentum and mandible size in larvae and decreased wing loading in adults. This study points out the deleterious effects of heavy metal exposure at various levels of biological organization and provides some clues regarding the mode of toxic action. This integrative approach provides new insights into the multi-level effects on aquatic insects exposed to heavy metal mixtures in field sediments, providing useful tools for ecological risk assessment in freshwater ecosystems.

© 2019 Elsevier Ltd. All rights reserved.

1. Introduction

Human activities release a wide range of chemical compounds into aquatic systems, and exposure to this complex mixture can affect the health of aquatic animals at the molecular, tissue, organ and whole organism level, even contributing to population decline (Floury et al., 2013; Vörösmarty et al., 2000). Insects are key elements for the functioning of freshwater ecosystems, as they sustain higher trophic levels and contribute to the carbon cycle in streams

and rivers. Certain developmental stages within their life cycle are particularly vulnerable to environmental stressors, and toxic exposures during these critical periods may have irreversible consequences (Weis, 2014). Indeed, early-life exposures could translate into phenotypic variations in adults, which can affect their fitness. In line with this, developmental abnormalities after exposure to chemical compounds have been reported in insects, particularly in chironomid larvae (Di Veroli et al., 2014; Martínez et al., 2003).

The current study focuses on the Oiartzun River (Basque Country, Spain), in the Natural Park of Aiako Harria. Study sites are located downstream the Arditurri mines, a complex of abandoned old Pb/Zn mines, characterized by a gradient of heavy metal contamination in sediments along the river (Méndez-Fernández,

* Corresponding author.

E-mail address: rplanello@ccia.uned.es (R. Planelló).

¹ Equal contribution to this paper.

2013; Basque Water Agency, 2016). Our aim was to investigate the effects of exposure of *Chironomus riparius* (Diptera, Chironomidae), a widely distributed insect in European freshwater ecosystems, to sediments contaminated with heavy metals. *C. riparius* (the two sexes) has an aquatic larval (developmental) stage and a terrestrial adult stage, which allows for its reproduction and dissemination. This species is widely used in the assessment of toxicity of water and sediments and four validated tests are included in the OECD Guidelines for the Testing of Chemicals (OECD, 2011, 2010, 2004a; 2004b). Given that molecular alterations have implications at larger scales in terms of morphology and physiology which may ultimately compromise population survival, we studied the toxic effects on different levels of biological organization ranging from molecular effects to the whole organism response. Unfortunately, few integrated and multilevel approaches studying toxic alterations in chironomids are available in the literature (Lee et al., 2018; Arambourou et al., 2019; Im et al., 2019). In this regard, and complementary to classical ecotoxicological endpoints, genetic biomarkers were proposed as early indicators of chemical toxicity. For example, transcriptional alterations of genes related to hormonal pathways, oxidative stress response, biotransformation metabolism (phase I and phase II) or DNA repair have been reported under different stress conditions (e.g. xenobiotic exposure, temperature) in laboratory and field studies with *C. riparius* (Herrero et al., 2016; Planelló et al., 2015). We also analyzed effects on respiration rates and on the lipid profile using ultra-high performance liquid chromatography/time-of-flight mass spectrometry. Given that it is often assumed that an animal's metabolic rate can be estimated through measuring the respiration rate (Salin et al., 2015), respiration rates were studied as a potential indicator of oxidative metabolism, since it is known that heavy metals can alter the metabolism of insects either by increasing detoxification pathways or by inhibiting key metabolic enzymes (Long et al., 2015). Taking into account that lipids can be mobilized for detoxification processes under toxic exposure and that heavy metals can induce lipid peroxidation, we hypothesize that the lipid profile will be disturbed by the heavy metal exposure.

Thus, through the use of *C. riparius* exposed to heavy metal-polluted sediments, our specific objectives were: i) to measure biochemical (lipidome analysis and transcriptional profile), physiological (respiration rate) and teratogenic (shape markers) effects; ii) to evaluate the relevance of life history traits (emergence rate, emergence time, and male-female ratio); and iii) to integrate multi-level responses.

2. Material and methods

2.1. Chironomid culture

The strain of *C. riparius* was maintained in the laboratory of ecotoxicology (IRSTEA) under a 16:8 h light:dark photoperiod at 20 ± 1 °C. Aquaria were composed of 2 cm of Fontainebleau sand layer (Fontainebleau sand Technical; VWR), surrounded by drill water (electrical conductivity = $450 \mu\text{S cm}^{-1}$; pH = 4.47; alkalinity = $219 \text{ mg HCO}_3^- \text{ l}^{-1}$), with constant oxygenation provided.

2.2. Study area and sampling methods

Two sites were studied in the Oiartzun River basin (Basque Country, Spain; Fig. 1): one reference (unpolluted) site (OIA) not affected by the mining activities; and one site downstream of the Ariturri mining district (ARD) (Table 1). The study area is located in the Paleozoic Cinco Villas Massif, west Aia granitic intrusion (Pesquera and Velasco, 1989), and rocks are rich in Pb, Zn, F and Ag ore deposits. Mining activities were carried out for about 2000

years, from Roman times until 1984 (Urteaga, 2008), and generated very large tailings heaps in the catchment of the Oiartzun River. Additionally, a sediment obtained from a large pool filled with groundwater at Iturbatz (ITU) (Entzia Mountains, Álava, Basque Country; Fig. 1) was included as a negative control (for physicochemical characterization see Méndez-Fernández et al., 2013).

At each study site, a composite sediment sample was taken from the upper layer (5–10 cm) of sediment deposits during the low water period on July 4th, 2017. After sifting the sediment through a 500- μm mesh to eliminate coarse particles and indigenous fauna (Reynoldson et al., 1994), 21 of the sample were obtained for sediment bioassays and chemical analyses of metal concentration. An unsifted subsample was also collected to gravimetrically determine the particle size distribution of the sediment, and the total organic content percentage (%TOC) was measured using the loss on ignition (LOI) method at 450 °C for 6 h (Bryan, 1985). Water physicochemical properties were measured at each site during the sampling day (Table 1).

2.3. Physicochemical characterization of the sediments

Seven metals (Cd, Cr, Cu, Hg, Ni, Pb, and Zn) and one metalloid (As) were quantified in the air-dried 63- μm sediment fraction (hereafter, we will refer to all these elements as “metals”). This sediment fraction was acid-digested using the microwave extraction method (USEPA, 2007) at the Technical Services of SGIker (UPV/EHU) and analyzed by ICP-MS (Agilent 7700X), or ICP-AES (Horiba Yobin Yvon Activa). The instrumental detection limits were: $0.001 \mu\text{g l}^{-1}$ As, $0.01 \mu\text{g l}^{-1}$ Cd, $0.07 \mu\text{g l}^{-1}$ Cr, $0.07 \mu\text{g l}^{-1}$ Cu, $0.03 \mu\text{g l}^{-1}$ Hg, $0.09 \mu\text{g l}^{-1}$ Ni, $0.06 \mu\text{g l}^{-1}$ Pb, and 0.04 mg l^{-1} Zn. The analytical batch included three replicates of the standard Buffalo River sediment (RM8704, USA) and Sewage Sludge-3 (SS3) as reference materials for quality control. The recovery rates for all metals were within certified values (76–105% for RM8704, and 83–106% for SS3). The metal sediment concentrations are reported on a dry weight basis ($\text{mg kg}^{-1} \text{ dw}$).

2.4. Experimental design of the bioassay

Glass jars were maintained at 16 ± 1 °C, under a 16:8 h light:dark photoperiod with constant oxygen supply. A 1.5-cm layer of field-collected sediments was provided as a substrate, and 4 vol of drill water was added. Water and sediment were left for 4 days to allow settlement of suspended solids. One hour before introduction of the larvae, overlying water was aerated, and measurements of the pH, temperature, conductivity, dissolved oxygen and nitrite were taken at day 0 and at subsequent 3-day intervals through the end of the test. Twenty newly hatched *C. riparius* larvae (1st stage) were introduced in each glass jar and fed daily *ad libitum* with 1 mg Tetramin® food per larva. The study design included 15 glass jars per condition ($n_{\text{total}} = 300$ larvae/condition); for each experimental condition, larvae from 9 jars were removed after 15 days of exposure for gene expression, lipidomic, respiration and shape analyses, while the other 6 jars were fitted with lids to retain emerging chironomids.

2.4.1. Studied endpoints

2.4.1.1. Mass measurement. Larvae were gently dried on a paper, pooled in groups of five individuals, and weighed using an ultramicrobalance (Sartorius Ultra Micro Balance MSU2.7S000DM; readability $0.1 \mu\text{g}$, repeatability $\pm 0.25 \mu\text{g}$).

2.4.1.2. Respiration rate. Larvae were left for 24 h in clean water to remove gut content. After that, 10 larvae were introduced into a glass jar containing a 1.5 cm sand layer surrounded by drill water.

Coordinates

Latitude,	Longitude	Site
42.818494,	-2.306469	Iturbatz
43.279505,	-1.820100	Oiartzun
43.283844,	-1.815604	Arditurri

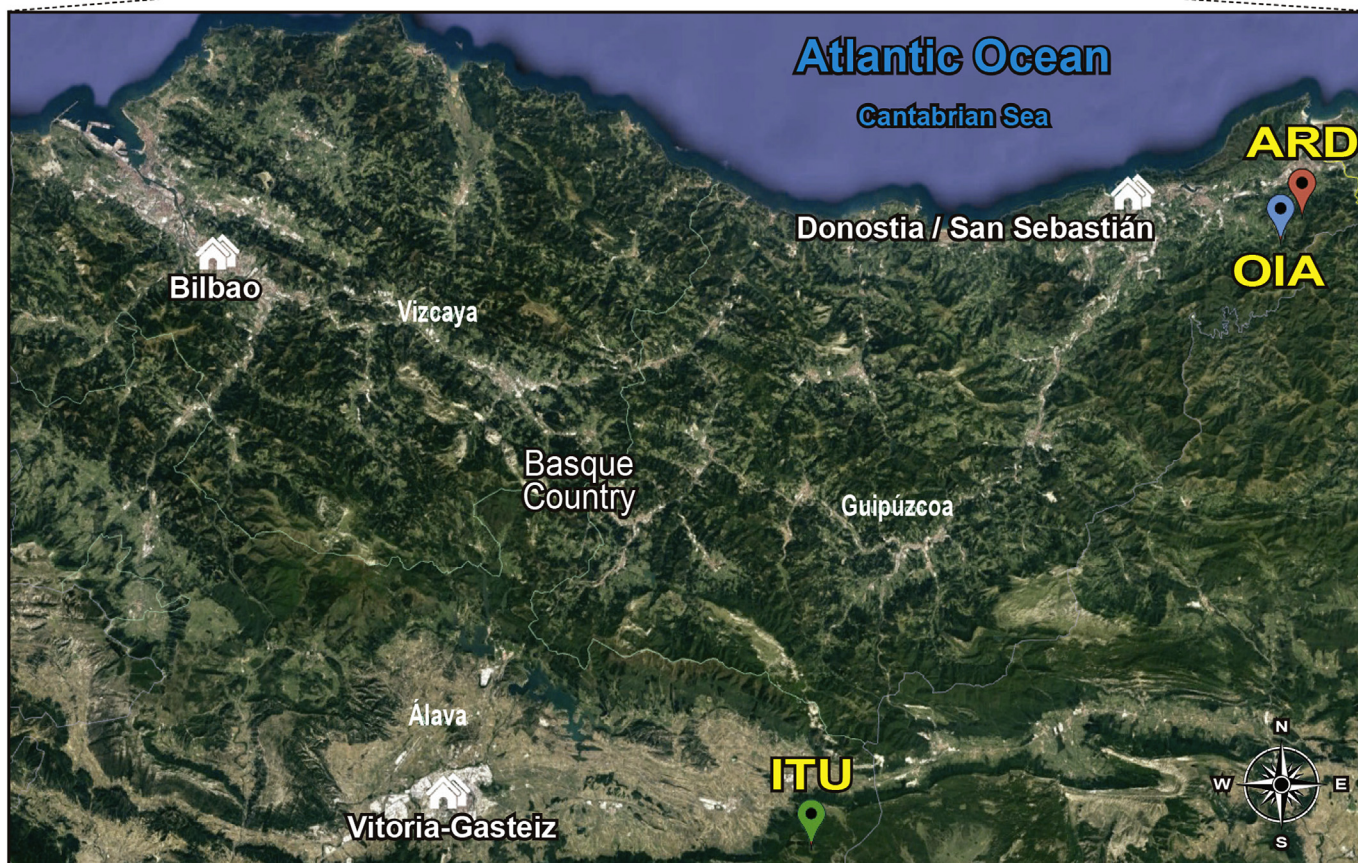


Fig. 1. Geographical localization of the three sampling sites in the Basque Country: ARD (Arditurri); OIA (Oiartzun); ITU (Iturbatz).

Jars were then hermetically sealed to allow CO₂ accumulation in the headspace. After 5 h, CO₂ content in the headspace was measured by gas chromatography. Four replicates per condition were tested, with a blank jar with no larvae also included. Respiration rate was expressed as ppm CO₂ min⁻¹ µg⁻¹ fresh mass.

2.4.1.3. Lipidomic analyses. Lipidomic analyses were performed as described by [Jordão et al. \(2015\)](#), with minor modifications. Larvae were normalized by mass to remove variation between conditions due to different larval growth. Five replicates, consisting of a pool of 5 normalized larvae, were analyzed per condition. Each replicate was homogenized in 1 ml of chloroform:methanol (2:1) with 2,6-di-*tert*-butyl-4-methylphenol (BHT; 0.01%) as an antioxidant, and lipid extraction was performed following a modified Folch method ([Folch et al., 1957](#)). Briefly, 100 µl of the homogenized sample was mixed with 750 µl of chloroform and 250 µl of methanol, and internal standards (pmol) were added ([Table S1](#)) for lipid semi-quantification. Samples were then dried under N₂, and lipid extracts were solubilized in 200 µl methanol. The LC-MS/MS consisted of a Waters Acquity UPLC system connected to a LCT premier

orthogonal accelerated time-of-flight mass spectrometer (Waters), operated in positive and negative ESI mode. Full-scan spectra from 50 to 1800 Da were obtained. Mass accuracy and reproducibility were maintained using an independent reference spray (Lock-Spray; Waters). An Acquity UPLC BEH C8, 100 mm × 2.1 mm, 1.7 µm (Waters) analytical column was used. A total of 200 lipids were identified and semi-quantified: 68 triacylglycerols (TAGs), 44 phosphatidylcholines (PCs), 23 phosphatidylethanolamines (PEAs), 21 diacylglycerols (DAGs), 14 phosphatidylserines (PSs), 11 lysophosphatidylcholines (LPCs), 9 sphingomyelins (SMs), 7 lysophosphatidylethanolamines (LPEAs) and 4 monoacylglycerols (MAGs).

2.4.1.4. Shape markers. Sixty head capsules were mounted on microscope slides using Eukitt® medium to present a ventral view, examined at 100× magnification on a Leica DM2000 LED microscope (Leica), and photographed with a Leica MC170 HD camera. Mentum deformities and mentum length fluctuating asymmetry were then evaluated as described in [Arambourou et al. \(2014\)](#). Deformity rate was calculated as the ratio of the number of individuals with deformed mouthparts to the number of examined

Table 1
Geographical information, physicochemical characteristics, sediment granulometry (distribution of gravimetric particle size), and metal composition of sediments collected in: ITU (Iturbatz; bioassay control), OIA (Oiartzun; reference site, unpolluted) and ARD (Arditurri; test site, contaminated). Abbreviations: Alt., site altitude; °C, temperature; k, water conductivity; O₂, dissolved oxygen in water; %SAT O₂, oxygen saturation; %TOC, Total Organic Content. Values for Threshold Effect Concentrations (TEC) and Probable Effect Concentrations (PEC) where obtained from McDonald et al. (2000). Grey cells indicate metal levels > PEC, while bold values indicate concentrations >10x PEC.

		ITU	OIA	ARD		
Geographical information	UTM-X	556,697	595,738	596,001		
	UTM-Y	4,740,896	4,792,511	4,793,075		
	Alt. (m)	1020	72	104		
Physico-chemical properties	pH	7.84	7.12	7.62		
	°C	12.8	14.8	21.6		
	k (μS cm ⁻¹)	464	81	128		
	O ₂ (mg l ⁻¹)	13.39	10.06	13		
	%SAT O ₂	141.7	100.3	149.6		
	%TOC	2.67	1.86	4.18		
Sediment granulometry	%2-1 mm	13.63	7.34	44.58		
	%1 mm-500μm	17.83	41.12	33.61		
	%500 μm-250μm	14.32	36.88	13.28		
	%250 μm-125μm	13.71	9.57	4.70		
	%125 μm-63μm	19.83	3.24	2.27		
	%<63 μm	20.68	1.87	1.57		
Metal concentration (mg kg ⁻¹)	As	18.2	8.39	53	9.79	33
	Cd	0.5	0.97	27.8	0.99	4.98
	Cr	26	48.4	40.7	31.6	149
	Cu	5.6	24.9	165	43.4	111
	Hg	0.04	0.18	1.87	0.18	1.06
	Ni	12.6	25.7	45.7	22.7	48.6
	Pb	16.3	85.8	1905	35.8	128
	Zn	53.3	336	11,221	121	459
					TEC	PEC

individuals. After emergence, adults were collected and sexed, their wings removed and placed on microscope slides in Eukitt® medium and then scanned using a Plustek OpticFilm 7400 scanner. Wing shape variations were measured by geometric morphometrics after digitizing 8 “type 1” landmarks, according to Arambourou et al. (2014). Wing area was calculated as the polygon delimited by the landmarks 1, 2, 3, 4, 5 and 8.

2.4.1.5. Gene expression analysis. Total RNA of 24 individuals (distributed among 6 independent experiments) was extracted using TRIzol Reagent (Invitrogen), following the manufacturer's protocol. After that, RNA was treated with RNase-free DNase (Roche, Germany) and extracted with phenol:chloroform:isoamyl alcohol (Fluka) using 5PRIME Phase Lock Gel Light tubes (QuantaBio). Purified RNA was resuspended in diethylpyrocarbonate (DEPC) water, quantified by spectrophotometry at 260 nm using a BioPhotometer (Eppendorf), and stored at -80 °C. For each condition and sample, 7 μg of isolated RNA was reverse-transcribed using Script Reverse Transcription Supermix (Bio-Rad), according to the manufacturer's instructions. The obtained cDNA was conserved at -80 °C and used as the template for subsequent qPCR analyses.

Transcriptional activity studies were carried out for a set of target genes, related to relevant metabolic processes: i) *EcR*, *InR*, *Vtg* (hormonal pathways); ii) *GST*, *GPx*, *SOD*, *CAT*, *TrxR1*, *cyp4G*, *FeH*, *FeL* (biotransformation and oxidative stress response); iii) *HbA*, *HbB*, *GAPDH* (oxygen transport and energy metabolism); iv) *hsp70*, *hsp40*, *hsp10*, *gp93* (stress response); and v) *NLK*, *XRCC1*, *ATM*, *DECAY* (DNA repair and apoptosis). Quantitative real-time RT-PCR (RT-qPCR) was carried out in a CFX96 Real-Time Detection System (Bio-Rad) using the Quantimix Easy Kit (Biotools, Spain). Genes encoding actin and the 26S ribosomal subunit were used as endogenous references. The statistical validation of the stability of the reference genes was performed by means of CFX Manager™ software, using an iterative test for pairwise variation according to Vandesompele et al. (2002).

The RT-qPCR was run as described in Herrero et al. (2018), with primer sequences shown in the supplementary material (Table S2). The mRNA level of each target gene was normalized against the expression of the two reference genes, and the $2^{-\Delta\Delta C_t}$ method was used to analyze relative changes in gene expression, using a CFX96 Real-Time Detection System and CFX Manager 3.1 software (Bio-Rad). Each sample was run in duplicate wells (technical replicates), and three biological replicates were performed for each experimental condition. Amplification efficiencies and correlation coefficients for each primer pair were calculated as described in Bio-Rad's Real-Time PCR Applications Guide (catalog #170-9799). For all genes, the efficiency of the assay was among 90–105% ($R^2 > 0.980$).

2.5. Statistical analysis

Statistical analyses were carried out using R 3.4.3 software (R Core Team, 2018). After checking data normality and homoscedasticity, differences in life history traits, biochemical markers (energy reserves) and normalized gene expression levels were evaluated using a non-parametric Kruskal Wallis test followed by a post hoc pairwise Mann-Whitney-Wilcoxon test. Differences in emergence time among the experimental conditions were analyzed using a Kaplan-Meier model. Lipids were grouped by family and compared among groups using one-way ANOVA. Mentum deformity rate variations were studied using a χ^2 proportion test. For length fluctuating asymmetry (FA) calculation, we used the FA10 index, which describes the average difference between sides after measurement error has been partitioned out (Palmer and Strobeck, 2003). Because FA10 is a variance estimate, we used F-tests to compare differences in FA among treatments (Palmer and Strobeck, 2003). Wing shape variation among treatment groups were analyzed by canonical variate analysis on Procrustes coordinates using MorphoJ software (Klingenberg, 2011). The Procrustes distance between each group was calculated and the significance was

assessed by a permutation test (10,000 permutations). A p value < 0.05 was used as the cutoff for statistical significance of differences among treatments.

3. Results

3.1. Physicochemical characteristics of water and sediments

The physicochemical characteristics of the water and sediments tested are shown in Table 1. Field water temperature ranged from 12.8 to 21.6 °C for the three sites, and high levels of dissolved oxygen in water were observed, ranging from 10.06 to 13.039 mg O₂ l⁻¹ (mean \pm sd = 12.15 \pm 1.82 mg O₂ l⁻¹), with 100.3–149.6% saturation (mean \pm sd = 130.5 \pm 26.5% saturation). Recorded pH values varied slightly and were considered natural for the study area, being neutral to slightly alkaline (range 7.12–7.84) (mean \pm sd = 7.53 \pm 0.37). Water electrical conductivity was low in the Oiartzun River basin, ranging from 81.0 to 464.0 μ S cm⁻¹ (mean \pm sd = 224.3 \pm 208.9 μ S cm⁻¹). The studied sediments had low-to-medium organic content (TOC = 1.86–4.18%) and were predominantly sandy, with a mean value at the three study sites of 8% silt-clay.

In the absence of Sediment Quality Guidelines (SQGs) in Spain, metal concentrations in sediments were evaluated using TEC (threshold effect concentration) and PEC (probable effect concentration) for North American freshwater sediments (MacDonald et al., 2000) (Table 1). The control site (ITU) showed metal concentrations about the same as the TEC values, except for As which was less than 1.1 times the TEC value. Metal contents in the studied ARD sediment were very high for Pb and Zn, with up to 1905 mg kg⁻¹ and 11,221 mg kg⁻¹, respectively (Table 1). The reference site, OIA, did not exceed the TEC values except for Cr, Ni, Pb, and Zn concentrations (1.5, 1.1, 2.3 and 2.7 times above the thresholds, respectively). In contrast, sediments from the test site located downstream of the abandoned mines (ARD) had concentrations which exceeded the PEC value for 6 of 8 metals, up to 14 times higher (14x) for Pb, 24x for Zn, and 5x for Cd. These metal concentrations therefore represent an environmental risk for aquatic communities (MacDonald et al., 2000).

3.2. Effects on *C. riparius*

3.2.1. Life history traits

Non-significant differences were observed in larval survival rate among the three studied sites (Table 2). However, there were significant differences in sublethal effects between larval and adult (both male and female), with the reduction of biomasses between ARD and ITU/OIA (Table 2). In addition, significant differences were observed between ARD and ITU regarding larval respiration rates and emergence rates (Table 2), and a delayed emergence in the ARD group of about 5 days for females and 4 days for males (Fig. 2 and

Table 2). Reduced dispersal among samples, depicted by the standard deviation, was observed for respiration rate in both OIA and ARD groups (Table 2).

3.2.2. Lipidomic analysis

Strong differences in the lipid profile were observed in ARD-treated larvae compared with those treated with ITU and OIA. Moreover, by comparison with both ITU and OIA groups, the dispersal among samples was higher in the ITU group (Fig. 3A). Although the total quantity of lipids did not differ among the three study groups, there were important differences in lipid composition among the groups, which are shown in the PCA (Fig. 3A) and heat map (Fig. 3B). The first axis of the PCA explained 38% of lipid variance, and the PC1 coordinates of the ARD group differed significantly from those of both ITU and OIA groups (ANOVA, $F_{2,12} = 48.7$, $p < 0.01$). The PC1 axis was positively correlated with some TAGs and unsaturated PCs while negatively correlated with some saturated SMs, saturated PCs, LPCs, LPEAs and TAGs (Fig. 3A).

The heatmap performed on the lipids contributing most to the first axis of the PCA showed a clear difference between the ARD group and ITU/OIA. In particular, the ARD group exhibited a higher content of TAGs and PCs (Fig. 3A).

PEA is the major component of phospholipids (about 55%), followed by PC (about 30%). Both the PC fraction and PC unsaturated/saturated ratio were significantly increased in the ARD group relative to ITU (Table 3). Furthermore, the PC/PEA ratio (membrane fluidity index) and general unsaturated/saturated ratios tended to increase in the ARD group (Table 3).

3.2.3. Shape markers

Relative to the ITU and OIA groups, both the mentum and the mandible lengths were significantly increased in the ARD group, with an observed higher variability in appendage length (Fig. 4A and B).

Length measurement error was lower than 15% for the mentum and lower than 23% for the mandibles, and no significant allometric effect was detected. As we detected slight side effects for the mentum in OIA and ARD groups, and for the mandible in the OIA group (Table 4), we cannot conclude that all the observed asymmetries in these groups were genuine FA. There was no significant difference in FA among the groups, neither for the mentum nor the mandibles.

The wing centroid size (Fig. 4C and D) was slightly reduced in males from the ARD group, with significant differences when compared to the OIA group. As a consequence of the mass decrease in the ARD group (Table 2), wing loading (Fig. 4E and F) calculated as the ratio between wing area and mean dry weight was sharply decreased in ARD males and females. The relationship between Procrustes coordinates and centroid size was significant in both males and females (permutation tests, $p < 0.05$), which suggested an allometric effect. To get rid of this allometry, for wing shape

Table 2

Measured life-cycle parameters. *: significantly different from ITU ($p < 0.05$).

	ITU	OIA	ARD
Larval survival rate (mean \pm sd) 9 replicates	85 \pm 4	86 \pm 5	93 \pm 6
Larval mass (mg \pm sd) 16 replicates of 5 pooled larvae	8.3 \pm 0.7	8.0 \pm 1.0	7.0 \pm 1.2*
Larval respiration rate (CO ₂ ppm min ⁻¹ μ g ⁻¹ \pm sd) 5 replicates	13.7 \pm 5.2	8.1 \pm 2.1	6.2 \pm 1.7*
Emergence rate (mean \pm sd) 6 replicates	79 \pm 7	88 \pm 14	92 \pm 7*
Male/female ratio (mean \pm sd) 6 replicates	1.2 \pm 0.6	1.0 \pm 0.4	1.2 \pm 0.8
Male emergence day (mean \pm sd)	23.7 \pm 1.5	23.6 \pm 1.7	27.4 \pm 1.9*
Female emergence day (mean \pm sd)	24.5 \pm 1.5	24.3 \pm 1.9	29.3 \pm 1.7*
Male mass (mg \pm sd) 6–10 replicates of 5 pooled males	0.93 \pm 0.08	0.99 \pm 0.05	0.49 \pm 0.04*
Female mass (mg \pm sd) 6–8 replicates of 5 pooled females	2.58 \pm 0.33	2.41 \pm 0.21	1.50 \pm 0.15*

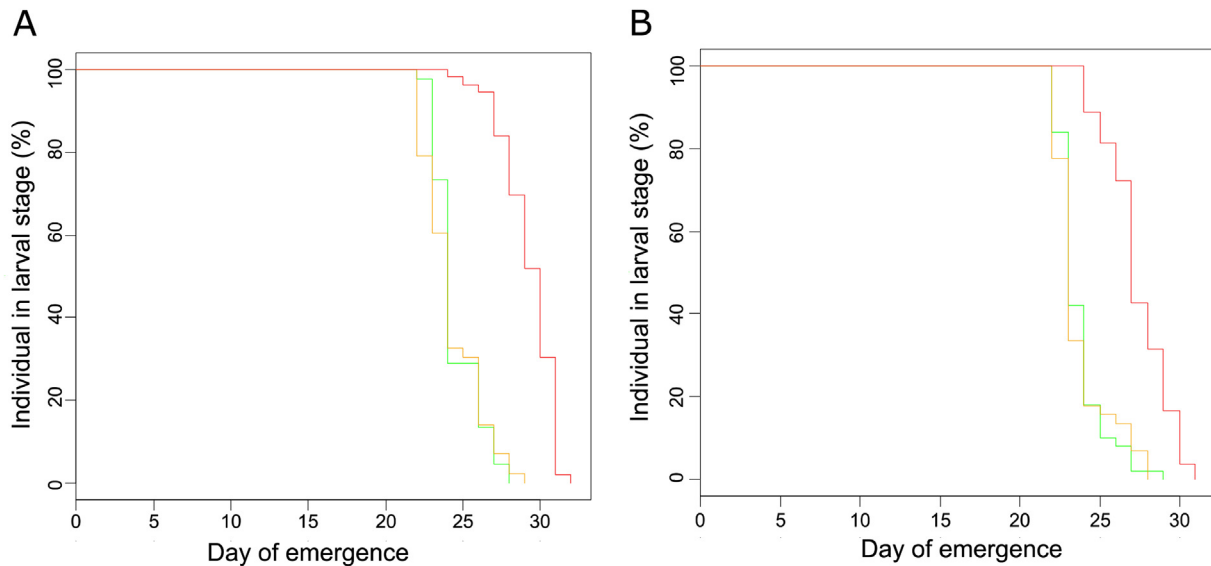


Fig. 2. Kaplan-Meier emergence curves for (A) female and (B) male *C. riparius* larvae treated with sediments collected from three different locations: ITU (Iturbatz; bioassay control; green), OIA (Oiartzun; reference site, unpolluted; orange) and ARD (Arditurri; test site, contaminated; red). (For interpretation of the references to colour in this figure legend, the reader is referred to the Web version of this article.)

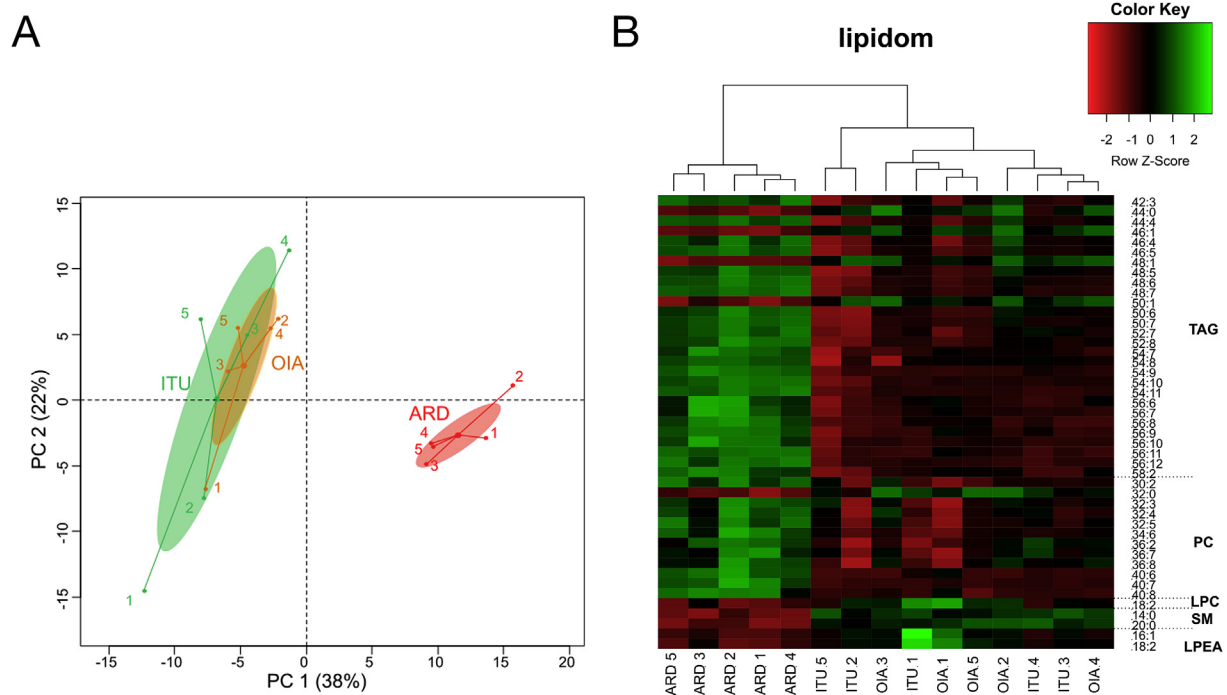


Fig. 3. PCA scores of the lipidome from larvae exposed to sediments from three sites: ITU (Iturbatz; bioassay control), OIA (Oiartzun; reference site, unpolluted) and ARD (Arditurri; test site, contaminated). (A) The two first components of the PCA together with sample scores are plotted, (B) A heatmap of lipids mostly contributing to the PC1. Hierarchical clustering analysis (represented as a heatmap) was performed using autoscale standardisation, Pearson's distance measure, and Ward's clustering algorithm. The colour key indicates the relative fold change across samples and lipid classes. TAG: triacylglycerols; PC: phosphatidylcholines; LPC: lysophosphatidylcholines; SM: sphingomyelins; LPEA: lysophosphatidylethanolamines. (For interpretation of the references to colour in this figure legend, the reader is referred to the Web version of this article.)

analysis we then used the residuals of the regression between shape and size. Canonical variate analysis on these residuals did not reveal any significant wing shape differences among groups neither for males nor for females (permutation tests on Procrustes distances, $p \geq 0.05$).

3.2.4. Gene expression analysis

Interesting dose-dependent alterations in the expression profiles were observed among the studied conditions. From a general perspective, most of the significant differences were observed in larvae exposed to the ARD sediment, compared to the OIA and ITU groups.

Table 3

Fraction of phospholipids and indexes of membrane fluidity (mean \pm sd) in larvae exposed to sediments from 3 sites: ITU (Iturbatz; bioassay control), OIA (Oiartzun; reference site, unpolluted) and ARD (Arditurri; test site, contaminated); *: significantly different from ITU ($p < 0.05$).

		ITU	OIA	ARD
Fraction of phospholipids	PEA	57.0 \pm 3.1	56.1 \pm 0.8	54.9 \pm 1.2
	PC	28.6 \pm 0.7	29.3 \pm 1.0	32.4 \pm 1.5*
	PS	11.0 \pm 0.7	11.1 \pm 0.3	10.6 \pm 0.3
	LPEA	2.0 \pm 1.4	2.0 \pm 0.6	1.2 \pm 0.3
	LPC	1.4 \pm 0.7	1.5 \pm 0.4	0.9 \pm 0.2
Indexes of membrane fluidity	Fluidity (PC/PEA)	0.50 \pm 0.04	0.52 \pm 0.02	0.59 \pm 0.04
	Unsaturated/saturated PEA	672 \pm 64	606 \pm 64	905 \pm 182
	Unsaturated/saturated PC	222 \pm 20	210 \pm 15	288 \pm 23*
	Unsaturated/saturated PS	29 \pm 3	29 \pm 2	30 \pm 2
	Unsaturated/saturated LPEA	4 \pm 1	4 \pm 1	5 \pm 2
	Unsaturated/saturated LPC	9 \pm 4	7 \pm 1	12 \pm 4

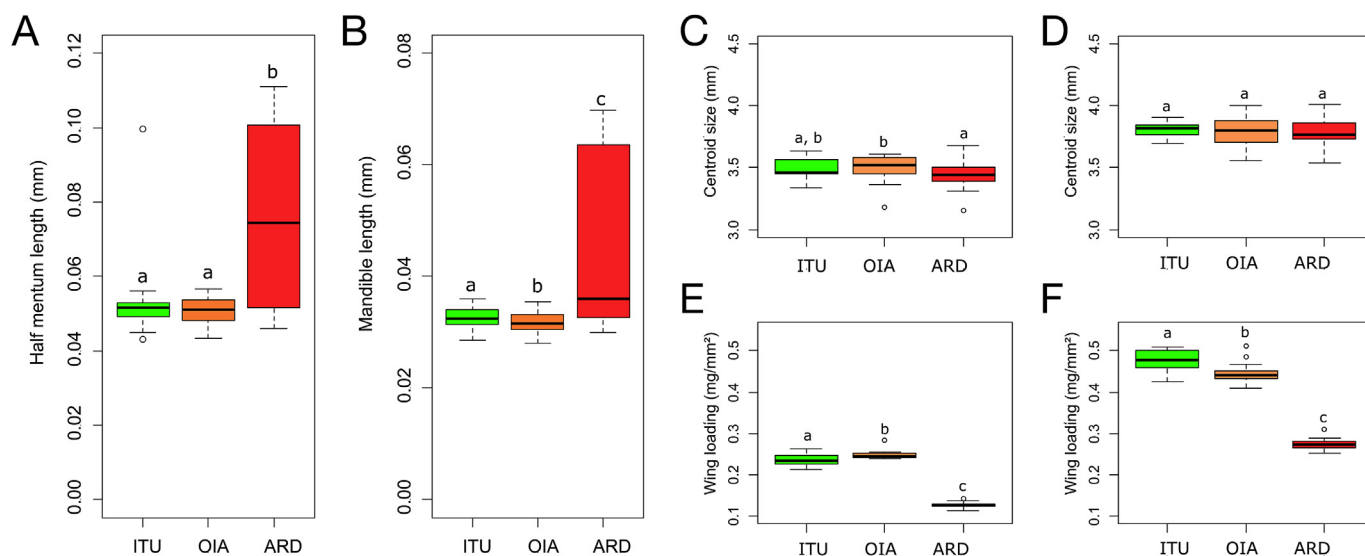


Fig. 4. Shape markers in larvae exposed to sediments from 3 sites: ITU (Iturbatz; bioassay control), OIA (Oiartzun; reference site, unpolluted) and ARD (Arditurri; test site, contaminated). (A) Mentum and (B) mandible lengths were measured (F test, all $p \geq 0.05$). Wing centroid size (mm) in (C) males and (D) females and wing loading (mg mm^{-2}) in (E) males and (F) females were compared among treatments. Different letters indicate significant differences (pairwise Mann Whitney Wilcoxon test).

Table 4

Deformity rates and FA affecting the mentum and the mandibles in the three study conditions: ITU (Iturbatz; bioassay control), OIA (Oiartzun; reference site, unpolluted) and ARD (Arditurri; test site, contaminated).

		ITU	OIA	ARD
Mentum	Deformity rate (%)	6	4	9
	FA index (10^{-2})	3.54	2.87	2.86
Mandible	Deformity rate (%)	12	4	8
	FA index (10^{-2})	2.7	2.83	2.65

Genes coding for the ecdysone and insulin receptors (*EcR* and *InR*) (Fig. 5A–B) were significantly down-regulated in larvae exposed to ARD sediments, with a mean decrease in transcription of 45% and 30%, respectively, relative to ITU. A similar (though not statistically significant) tendency was also observed in the *vtg* gene (Fig. 5C).

Regarding biotransformation and detoxification processes, genes were differentially affected depending on the condition, with a decreasing mRNA abundance among field sediments. The transcription of *GST* and *SOD* genes showed similar responses to those observed for hormone-related genes, with a significant down-regulation in ARD samples compared to ITU (Fig. 5D, F). However, in the case of *GPx*, *CAT*, and *TrxR1*, OIA samples were significantly repressed (up to 40% for *CAT*) (Fig. 5E, G–H), with no changes for

ARD. ARD sediments reduced the transcript levels of *cyp4g*, showing similar effects to those observed for *EcR* and *InR* (significant when compared to OIA) (Fig. 5I). These repressions reached values of 47% for *GST*, 30% for *SOD* and 20% for *cyp4g*, when compared to the ITU control group. In the case of genes coding for ferritins (Fig. 5J–K), a completely different effect was observed, consisting of strong overexpression in ARD samples (3.5-fold for *FeH* and 2.1-fold for *FeL* with respect to ITU; significant for *FeL*).

Genes related to oxygen transport (*HbA* and *HbB*) responded differentially across the studied sediment samples (Fig. 6A–B). A strong and significant up-regulation of *HbB* was observed for ARD (41 and 9-fold compared to ITU and OIA, respectively), while *HbA* remained unaltered. *GAPDH* stayed constant among larvae from the three studied conditions (Fig. 6C).

The transcription of genes involved in the cell stress response (*hsp70*, *hsp40*, *hsp10*, *gp93*) showed different patterns. In the ARD group, *hsp10* and *gp93* (Fig. 6F–G) showed an increase (up to 2-fold) in transcription, whereas OIA samples had a repression of around 50% compared to ITU (significant for *hsp10*). In contrast, *hsp70* and *hsp40* remained unchanged (Fig. 6E–F).

Finally, no differences were detected in the expression profiles of DNA repair and apoptosis genes (Fig. 6H–K), although there was remarkable variability in the transcription of the *DECAY* and *ATM* genes in larvae exposed to ARD sediments.

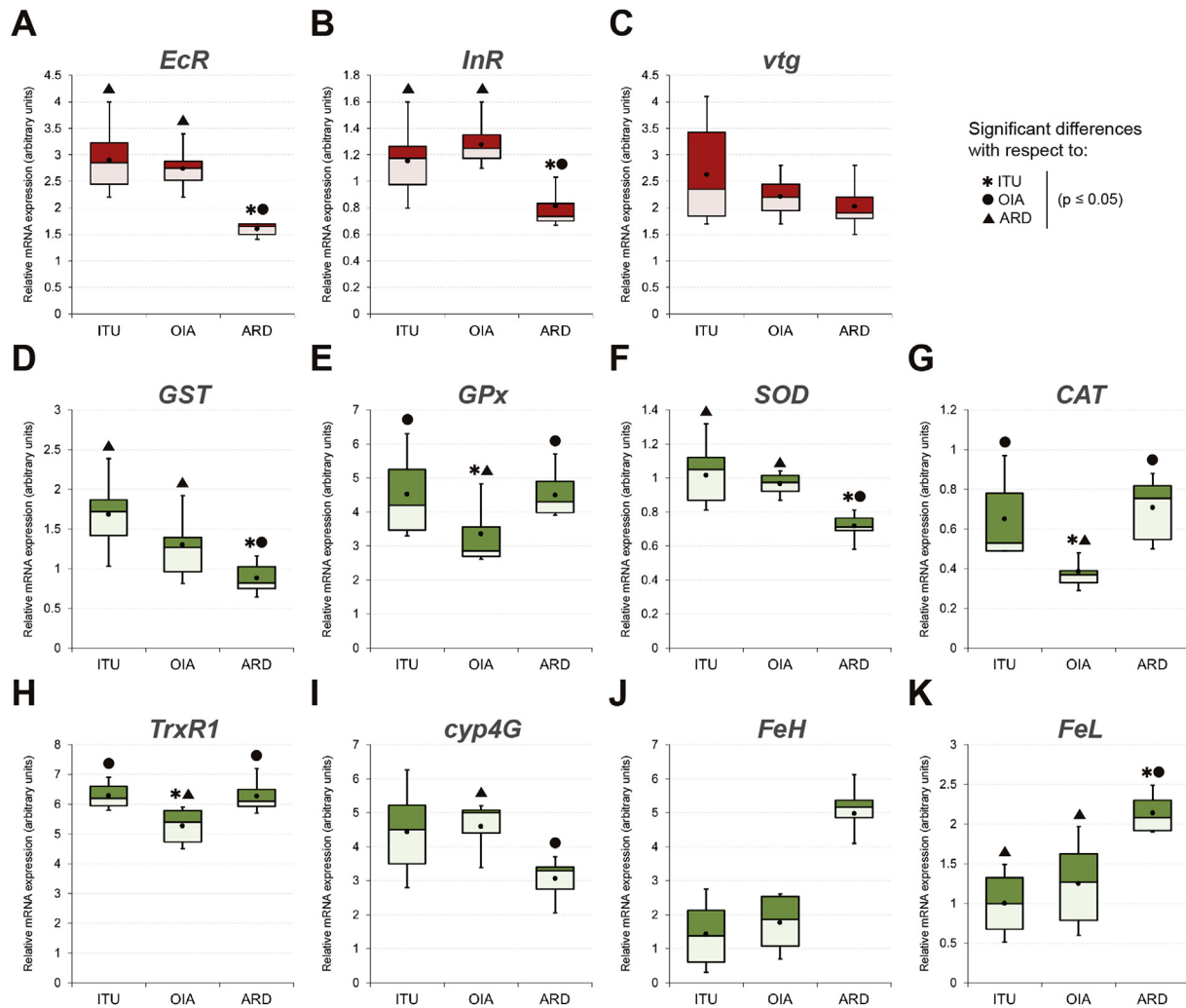


Fig. 5. Changes in expression of genes related to hormonal pathways, biotransformation and oxidative stress response in *C. riparius* 4th instar larvae exposed to sediments from 3 sites: ITU (Iturbatz; bioassay control), OIA (Oiartzun; reference site, unpolluted) and ARD (Arditurri; test site, contaminated). Box-and-whisker plots represent the expression patterns of the studied genes measured by real-time RT-PCR: (A) *EcR*; (B) *InR*; (C) *vtg*; (D) *GST*; (E) *GPx*; (F) *SOD*; (G) *CAT*; (H) *TrxR1*; (I) *cyp4G*; (J) *FeH*; and (K) *FeL*. For each experimental condition, six independent experiments were performed, and RNA was extracted from groups of 6 larvae ($n = 24$). Box and whiskers represent the 25–75 percentile and the minimum/maximum measured values, respectively; the mean is represented by a dot, whereas the horizontal line separating the lower (dark) and the upper (light) area represents the median.

4. Discussion

Mining activity in areas close to particularly sensitive environments such as aquatic ecosystems is currently of special concern. It is necessary to elucidate the mechanisms responsible for the observed effects in order to better understand the ecological impacts of mining on stream ecosystems (Besser et al., 2009). However, few studies have exhaustively evaluated medium and long-term multilevel responses caused by complex polluted sediments in natural biota (Arambourou et al., 2019). Thus, the aim of this work was to evaluate the potential toxicity of high levels of heavy metal contamination in sediments near a mining area, using the key species *C. riparius*. This species is widely used as an *in vitro* model for the evaluation of toxic effects of environmental contaminants. We used an integrative approach based on response patterns observed in this species, from the molecular to the organism level, which may also be applied to environmental risk assessment processes. The present study demonstrated that exposure to water/sediments contaminated by heavy metals resulted in reproduction and growth impairment, respiration

reduction, morphometric and allometric changes, differential accumulation of storage lipids (i.e. TAGs) and some glycerophospholipids (PCs), as well as alterations in gene expression in *C. riparius*.

The delayed emergence seen in both males and females exposed to metal contaminated ARD sediments has been widely observed in chironomids exposed to contaminated sediments (Arambourou et al., 2014), and might be due to a higher energy investment necessary to counteract toxic stress, with a consequent decrease in growth. Moreover, the endocrine disrupting activity could be also responsible for these effects (Planelló et al., 2010; Cao et al., 2019), given the observed alterations in some of the genes related to hormonal pathways (Fig. 5A–C). The expression of the ecdysone receptor gene (*EcR*)—a well-known biomarker of endocrine disruption—and the insulin receptor (*InR*) were analyzed as they are two key genes involved in the control of insect development. Exposure to ARD sediments led to downregulation of both genes, suggesting that contaminants can prevent the action of these hormones, possibly disrupting their genetic signaling cascades. The interaction between insulin and ecdysteroid signaling pathways are

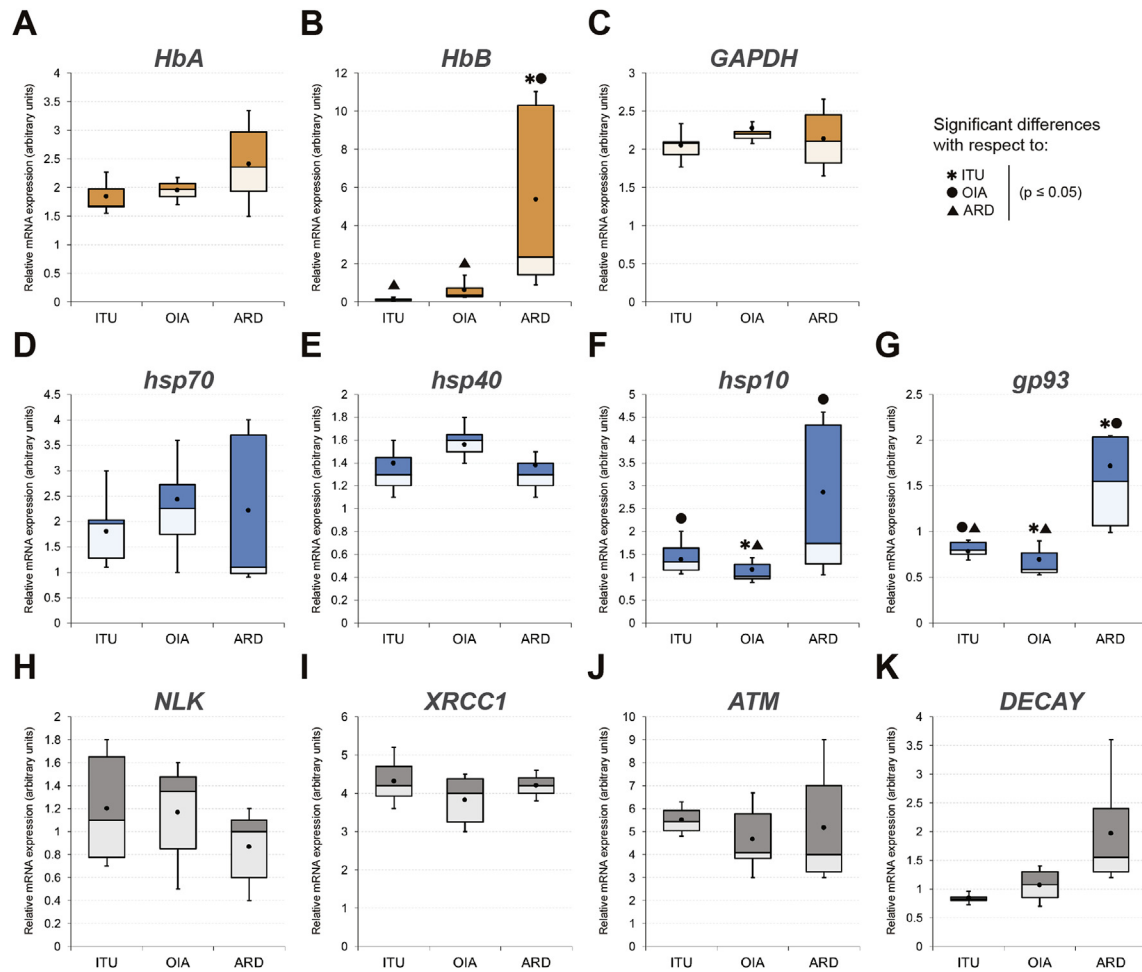


Fig. 6. Changes in expression of genes related to oxygen transport, cell stress response and DNA repair/apoptosis in *C. riparius* 4th instar larvae exposed to sediments from 3 sites: ITU (Iturbatz; bioassay control), OIA (Oiartzun; reference site, unpolluted) and ARD (Arditurri; test site, contaminated). Box-and-whisker plots represent the expression patterns of the studied genes measured by real-time RT-PCR: (A) *HbA*; (B) *HbB*; (C) *GAPDH*; (D) *hsp70*; (E) *hsp40*; (F) *hsp10*; (G) *gp93*; (H) *NLK*; (I) *XRCC1*; (J) *ATM*; and (K) *DECAF*. For each experimental condition, six independent experiments were performed, and RNA was extracted from groups of 6 larvae ($n = 24$). Box and whiskers represent the 25–75 percentile and the minimum/maximum measured values, respectively; the mean is represented by a dot, whereas the horizontal line separating the lower (dark) and the upper (light) area represents the median.

essential for fine control of tissue and body growth (Lin and Smaghe, 2018). It is noteworthy that larvae were lighter in the ARD group than in the other groups, suggesting decreased growth. Moreover, alterations in the ecdysone pathway could ultimately affect ecdysteroids such as 20-hydroxyecdysone, the active form of ecdysone which controls molting and metamorphosis in insects (Henrich et al., 1999).

The reproductive success of all species, including insects, relies on vitellogenin biosynthesis and its uptake in developing oocytes. Ecdysteroids also regulate vitellogenin in the fat body throughout a conserved set of ecdysone-responsive early and early-late genes (Swevers and Iatrou, 2009). The concomitant downregulation observed in the vitellogenin gene (*vtg*) demonstrates that the heavy metal mixture present in ARD sediments affected downstream the ecdysone signaling pathway. Given that vitellus is the main energy source that fuels embryo development, this may result in significant reproductive impairment (Roy et al., 2007) that affects embryogenesis of the subsequent generation due to a reduction of yolk synthesis and egg production. Our results are in accordance with the reduction of vitellogenin previously described in insects (Cervera et al., 2006; Su et al., 2019; Zhao et al., 2016), crustaceans (Yang et al., 2015), mollusks (Moncaleano-Niño et al., 2017), and

fish (Driessnack et al., 2017a, 2017b) exposed to heavy metals (Cd, Pb, etc.).

Besides the reproductive modifications, imbalances in normal physiological and metabolic activities were also critical factors in the stress response induced by ARD sediments, including a significant decrease in respiration rate. Respiration has also been shown to decrease in *Chironomus* sp. after exposure to thiacloprid (Langer-Jaesrich et al., 2010), zinc (Miller and Hendricks, 1996), or naphthalene (Darville and Wilhm, 1984). The decrease in oxygen uptake might be caused by a disruption of the electron transport chain, as observed in *C. riparius* exposed to $20 \mu\text{g l}^{-1}$ fenitrothion (Choi et al., 2000), or linked to a decrease in locomotive activity, as observed in *C. riparius* exposed to mercury (Azevedo-Pereira and Soares, 2010). This physiological imbalance was in accordance with one of the most remarkable alterations caused by exposure to contaminated sediments at the genetic level, observed in the activity of the *HbB* gene, with up to a 41-fold increase in its transcription. This specific induction might be: 1) a rapid response to mitigate oxygen deficits arising from the decrease in respiration rate; or 2) the result of an increased oxygen demand for xenobiotic metabolism processes. It is known that *Chironomus* hemoglobins (Hbs) show a strong affinity for oxygen and a extracellular

localization, and their expression is considered to be a sensitive biomarker after exposure to different pollutants, such as metals or pesticides (Ha and Choi, 2008; Lee et al., 2006). Our results agree with the idea that the presence of Hbs in invertebrates implies the evolutionary adaptation of these organisms to unfavorable environmental conditions, because these pigments help sustain aerobic metabolism when oxygen availability is limited (Osmulski and Leyko, 1986).

Regarding the lipidomic profile, TAGs, which are important components of storage lipids (Kühnlein, 2012), were significantly increased in the group exposed to contaminated sediments, and PC, which is an important component of cell membranes (Gilbert and O'Connor, 2012; Dobrosotskaya et al., 2002), was also increased. Two hypotheses could explain this result. First, it may be related to respiration decrease and growth rate inhibition; since TAGs are partly used to generate energy through cellular respiration, a decrease in respiration rates could contribute to an increase in their levels (Kühnlein, 2012). Also, phospholipids are important components of cell membranes and arthropod carapaces (Gilbert and O'Connor, 2012), so animals with reduced growth could accumulate non-invested glycerophospholipids. Secondly, TAGs have been shown to be implicated in the antioxidant response, limiting the level of reactive oxygen species (ROS) and inhibiting the oxidation of polyunsaturated fatty acids in *Drosophila* stem cells (Bailey et al., 2015). Therefore, TAGs might increase as a way to prevent oxidative damages in exposed individuals. Reduced dispersal among samples in the ARD-treated group was observed for respiration rate and lipid profile, as reported by Wheelock et al. (2005) for enzyme activity in salmon exposed to esfenvalerate. Toxic exposure could first affect the most sensitive individuals leading to a narrower response in the most contaminated sediment.

In accordance with *Drosophila* literature (Carvalho et al., 2012; Scheitz et al., 2013), PEAs are the major component of phospholipids. A decrease in lipid saturation, summarized by the unsaturated/saturated ratio, is associated with reduced membrane fluidity, and membranes containing a low proportion of PEAs are also said to be rigid. Our results suggest a decrease of membrane fluidity in the larvae exposed to contaminated sediment, consistent with decreases previously reported in cells exposed to heavy metals (García et al., 2005). This might be due to lipid peroxidation (LPO) in the phospholipid bilayer, which has been shown to increase membrane rigidity (Dobretsov et al., 1977). Moreover, metals may bind phospholipids and alter surface charge structures and lipid conformation (Tocanne and Teissié, 1990) leading to an increase of the membrane rigidity (García et al., 2005). An increase in membrane rigidity has been reported to be correlated to a higher resistance to toxic exposure in *Drosophila* (Scheitz et al., 2013), thus we can hypothesize that increased membrane rigidity might also protect cells from metal uptake. Metals may also enter or be excreted through membrane transporters. For example, in *Drosophila*, the ABC transporters which are transmembrane proteins were shown responsible for zinc and copper detoxification (Yepiskoposyan et al., 2006).

Exposure to contaminated sediment induced allometric changes; length of appendages (mentum and mandible) was enhanced while larval mass was reduced. Appendage size increase has been observed in crustaceans exposed to compounds with juvenoid activity (Arambourou et al., 2017; Olmstead and LeBlanc, 2000) and to sewage treatment works (Gross et al., 2001). To the best of our knowledge, this is the first time that this effect has been observed in response to heavy metal exposure, and it may result either from alteration of the regulatory pathways controlling appendage formation, endocrine disruption activity (Mamon et al., 2016), or by differences in appendage wear in relation to the size of sediment particles (Bird, 1997). The latter hypothesis does not seem

very likely, as the grain size distribution of the OIA and ARD sediments was quite similar (86% and 94%, respectively, of particles with a diameter greater than 250 μm). Given that adult mass was severely reduced with little effect on wing size, wing loading was sharply decreased in both males and females exposed to ARD sediments. A positive relationship between wing loading and flight performance has been observed in butterflies (Lin and Smagghe, 2018). Thus, the wing loading decrease might have dramatic repercussions on flight performance and, as a consequence, reproductive success and species dispersal.

At a molecular level, the expression profiles of other genes were affected by exposure to contaminated sediments, especially those involved in cell stress response, biotransformation metabolism, and response to oxidative stress.

Heat-shock proteins (HSPs) are naturally induced by stress and abnormal conditions, and thus can be useful indicators of stress in a variety of organisms and under different circumstances. The *hsp10*, *hsp40*, *hsp70* and *gp93* genes were selected as biomarkers of cellular stress response. Especially remarkable was the induction observed in the activity of *gp93*, which encodes the ortholog of the endoplasmic reticulum resident HSP90, whose expression enables nutrient assimilation-coupled growth control (Maynard et al., 2010). *gp93* mutant larvae exhibit a starvation-like metabolic phenotype, including suppression of insulin signaling and extensive mobilization of amino acids and triglycerides. Visual comparisons of *gp93* mutant larvae have indicated that loss of *gp93* expression results in a late larval growth defect (Maynard et al., 2010). Our results showed that both *InR* and *gp93* genes had opposite responses. *gp93* induction could be interpreted as a larval response to hormonal receptor disruption caused by heavy metals and the deleterious effects on larval weight, in an attempt to increase nutrient assimilation.

HSP70 and HSP40 play a crucial role in protein folding and protein homeostasis. Moreover, HSP40 stimulates the ATPase activity of HSP70 and regulates protein folding, unfolding, translation, translocation, and degradation. In addition, HSP70 is a necessary component for the correct function of the EcR (Gilbert et al., 2002). The transcriptional activity of both *hsp70* and *hsp40* have been shown to be modulated by exposure to different xenobiotics. Previous studies described the induction of *hsp70* in *C. riparius* exposed to paraquat dichloride, chlorpyrifos, fenitrothion, cadmium chloride, lead nitrate, potassium dichromate or bisphenol A (Lee et al., 2006; Planelló et al., 2008). In contrast to this, our results showed constant levels of *hsp70* in all the experimental conditions. This may be due to the fact that HSP70 is involved in a variety of processes related to the maintenance of cellular homeostasis (Murphy, 2013), and thus might not be affected only by the effects described for the nuclear receptors.

To protect against the effects of pollutants and oxidative stress, organisms have a variety of detoxifying enzymes, such as superoxide dismutase (SOD), catalase (CAT), glutathione-S-transferase (GST), or glutathione peroxidase (GPx), among others (Felton and Summers, 1995). Our results showed that exposure to metals caused significant changes in the transcriptional profile of GST and SOD. Meanwhile, significant downregulation of GPx, CAT and *TrxR1* was detected only in the OIA group. Our results are in accordance with the induction of oxidative stress-mediated genotoxicity, described in *D. melanogaster* under Pb exposure (Olakkaran et al., 2018). Pb, which in our study was highly present in the ARD sediments, has been shown to induce oxidative stress by overproducing ROS, LPO, and decrease of antioxidant enzymes such as SOD, CAT, and GST, as well as wing somatic mutation (Olakkaran et al., 2018). This response is especially interesting, since it contrasts with the induction of defense mechanisms described in insects, including *C. riparius*, after exposure to multiple xenobiotics (Martínez-Paz,

2018; Nair et al., 2013, 2011; Nikolić et al., 2016).

Ferritin proteins (Fe) have been described to function as iron transporters, and recently they have been shown to play additional roles as a cytotoxic protector against oxidative challenges and in the immune response (Pham and Winzerling, 2010). Insect ferritins are composed of two types of subunits (FeH and FeL) homologues to vertebrates (Georgieva et al., 1999). In this study, both *FeH* and *FeL* genes of *C. riparius* were upregulated in larvae exposed to the ARD sediments. This is consistent with previous results obtained in *D. melanogaster* (Missirlis et al., 2007) and *C. riparius* (Park et al., 2010) after exposure to paraquat and 2,4-dichlorophenoxyacetic acid, respectively, and may lead to protection responses against induced oxidative damage of these herbicides. Given the high levels of Pb in the ARD point, ferritin upregulation could be also part of an antioxidant mechanism against oxidative stress induced by lead.

No significant variations were detected in the activity of *GAPDH*, which remained constant under our three experimental conditions. This is consistent with the traditional use of this gene as a reference “housekeeping” gene in transcriptional studies, though it has been demonstrated that its expression may sometimes be altered under xenobiotic-induced stress (Herrero et al., 2017).

Taking into account the alterations observed in shape markers (mouthpart and wings), and the transcriptional depletion of antioxidant genes, the potential genotoxic damage was evaluated through the transcriptional activity of genes closely related to DNA repair and apoptosis. No significant changes in transcript levels of these genes were detected; however, the slight increase in *DECAY* and downregulation of *NLK* may indicate a reduction in DNA repair rates and the induction of apoptosis as a consequence of indirect DNA damage, which may lead to genotoxic damage. Genotoxicity of heavy metals has been described in chironomids at different levels; somatic chromosome aberrations are sensitive indicators of genotoxicity of trace metals in some aquatic dipterans (Ilkova et al., 2018). DNA damage induced by Cu was reported by Bernabò et al. (2017), and downregulation of DNA repair genes has been described after vinclozolin exposure due to high DNA damage and the failure of cellular repair mechanisms (Aquilino et al., 2018). In this regard, more detailed studies should be conducted to evaluate the genotoxic risk of these complex mixtures of metals.

5. Conclusions

This study with the midge *C. riparius* highlights the effects of exposure to heavy metal-contaminated sediments from the mining area of Arditurri (Basque Country). The selected biomarkers allowed us to integrate biological responses at different time scales, while the multidisciplinary approach included several levels of biological organization, from the molecular to the whole organism response. Exposure to complex mixtures of heavy metals disrupted the activity of hormone-related genes, and impaired reproduction and growth in *C. riparius* larvae and adults, which may affect long-term population dynamics of this key species for aquatic ecosystems. Exposed individuals also shown an altered activity of genes related to detoxification processes and oxidative stress, which could lessen their biotransformation rates and their ability to prevent oxidative damage. Through these biomarkers, this integrative assay offers useful information about molecular, physiological, reproductive, and morphological alterations observed in natural polluted scenarios. Combining classical toxicity parameters with molecular tools, chemical analysis, and bioinformatics, could lead us to more robust environmental risk assessments, and to a better understanding of the risks that mining activity can bring to aquatic biota.

Declaration of competing interest

The authors declare that they have no known competing financial interests or personal relationships that could have appeared to influence the work reported in this paper.

Acknowledgements

The professional editing service NB Revisions was used for technical preparation of the text prior to submission.

Appendix A. Supplementary data

Supplementary data to this article can be found online at <https://doi.org/10.1016/j.watres.2019.115165>.

Funding

This research was supported by the National Distance Education University (UNED) through the 2018I/PPRO/008 project, and the Spanish Ministry of Economy and Competitiveness (MINECO) through the CGL 2013-44655-R and CTM 2017-83242-R research projects. Lola Llorente was co-financed by the Community of Madrid Government and the European Social Fund with a research assistant contract (PEJ-2017-AI/BIO-6834). Iñigo Moreno-Ocio was supported by a predoctoral fellowship from the University of the Basque Country (UPV/EHU). Dr. Leire Méndez-Fernández was financed by the project “Ecosystem Services Assessment of the Basque Country” funded by contract agreement with the Department of Environment and Regional Planning of the Basque Government (CONV18/01) and the Department of Sustainability and Environment of Biscay Provincial Council (CONV15/08).

References

- Aquilino, M., Sánchez-Argüello, P., Martínez-Guitarte, J.-L., 2018. Genotoxic effects of vinclozolin on the aquatic insect *Chironomus riparius* (Diptera, Chironomidae). *Environ. Pollut.* 232, 563–570. <https://doi.org/10.1016/j.envpol.2017.09.088>.
- Arambourou, H., Beisel, J.-N., Branchu, P., Debat, V., 2014. Exposure to sediments from polluted rivers has limited phenotypic effects on larvae and adults of *Chironomus riparius*. *Sci. Total Environ.* 484, 92–101. <https://doi.org/10.1016/j.scitotenv.2014.03.010>.
- Arambourou, H., Chaumot, A., Vulliet, E., Daniele, G., Delorme, N., Abbaci, K., Debat, V., 2017. Phenotypic defects in newborn *Gammarus fossarum* (Amphipoda) following embryonic exposure to fenoxycarb. *Ecotoxicol. Environ. Saf.* 144, 193–199. <https://doi.org/10.1016/j.ecoenv.2017.06.017>.
- Arambourou, H., Planelló, R., Llorente, L., Fuertes, I., Barata, C., Delorme, N., Noury, P., Herrero, Ó., Villeneuve, A., Bonninau, C., 2019. *Chironomus riparius* exposure to field-collected contaminated sediments: from subcellular effect to whole-organism response. *Sci. Total Environ.* 671, 874–882. <https://doi.org/10.1016/J.SCITOTENV.2019.03.384>.
- Azevedo-Pereira, H.M.V.S., Soares, A.M.V.M., 2010. Effects of mercury on growth, emergence, and behavior of *Chironomus riparius* Meigen (Diptera: chironomidae). *Arch. Environ. Contam. Toxicol.* 59, 216–224. <https://doi.org/10.1007/s00244-010-9482-9>.
- Bailey, A.P., Koster, G., Guillermier, C., Hirst, E.M.A., MacRae, J.I., Lechene, C.P., Postle, A.D., Gould, A.P., 2015. Antioxidant role for lipid droplets in a stem cell niche of *Drosophila*. *Cell* 163, 340–353. <https://doi.org/10.1016/j.cell.2015.09.020>.
- Basque Water Agency, 2016. Plan Hidrológico. Parte Española de la Demarcación Hidrográfica del Cantábrico Oriental. Revisión 2015-2021, p. 177. https://www.uragentzia.euskadi.eus/contenidos/informacion/documentacion_plan_2015_2021/es_def/adjuntos/20151214/01_MEMORIA%20Cantabrico%20Oriental.pdf.
- Bernabò, P., Gaglio, M., Bellamoli, F., Viero, G., Lencioni, V., 2017. DNA damage and translational response during detoxification from copper exposure in a wild population of *Chironomus riparius*. *Chemosphere* 173, 235–244. <https://doi.org/10.1016/j.chemosphere.2017.01.052>.
- Besser, J.M., Brumbaugh, W.G., Allert, A.L., Poulton, B.C., Schmitt, C.J., Ingersoll, C.G., 2009. Ecological impacts of lead mining on Ozark streams: toxicity of sediment and pore water. *Ecotoxicol. Environ. Saf.* 72, 516–526. <https://doi.org/10.1016/j.ecoenv.2008.05.013>.
- Bird, G.A., 1997. Deformities in cultured *Chironomus tentans* larvae and the influence of substrate on growth, survival and mentum wear. *Environ. Monit. Assess.* 45,

- 273–283. <https://doi.org/10.1023/A:1005782803930>.
- Bryan, G.W., 1985. A Guide to the Assessment of Heavy-Metal Contamination in Estuaries Using Biological Indicators. Marine Biological Association of the U.K., Plymouth, England.
- Cao, J., Wang, G., Wang, T., Chen, J., Wenjing, G., Wu, P., He, X., Xie, L., 2019. Copper caused reproductive endocrine disruption in zebrafish (*Danio rerio*). Aquat. Toxicol. 211, 124–136. <https://doi.org/10.1016/j.aquatox.2019.04.003>.
- Carvalho, M., Sampaio, J.L., Palm, W., Brankatschk, M., Eaton, S., Shevchenko, A., 2012. Effects of diet and development on the *Drosophila* lipidome. Mol. Syst. Biol. 8, 600. <https://doi.org/10.1038/msb.2012.29>.
- Cervera, A., Maymó, A.C., Martínez-Pardo, R., Garcerá, M.D., 2006. Vitellogenin polypeptide levels in one susceptible and one cadmium-resistant strain of *Oncopeltus fasciatus* (Heteroptera: lygaeidae), and its role in cadmium resistance. J. Insect Physiol. 52, 158–168. <https://doi.org/10.1016/j.jinsphys.2005.10.001>.
- Choi, J., Roche, H., Caquet, T., 2000. Effects of physical (hypoxia, hyperoxia) and chemical (potassium dichromate, fenitrothion) stress on antioxidant enzyme activities in *Chironomus riparius* mg. (diptera, chironomidae) larvae: potential biomarkers. Environ. Toxicol. Chem. 19, 495–500. <https://doi.org/10.1002/etc.5620190231>.
- Darville, R.G., Wilhm, J.L., 1984. The effect of naphthalene on oxygen consumption and hemoglobin concentration in *Chironomus attenuatus* and on oxygen consumption and life cycle of *Tanytarsus dissimilis*. Environ. Toxicol. Chem. 3, 135–141. <https://doi.org/10.1002/etc.5620030115>.
- Di Veroli, A., Santoro, F., Pallottini, M., Selvaggi, R., Scardazza, F., Cappelletti, D., Goretti, E., 2014. Deformities of chironomid larvae and heavy metal pollution: from laboratory to field studies. Chemosphere 112, 9–17. <https://doi.org/10.1016/j.chemosphere.2014.03.053>.
- Dobretsov, G.E., Borschevskaya, T.A., Petrov, V.A., Vladimirov, Y.A., 1977. The increase of phospholipid bilayer rigidity after lipid peroxidation. FEBS Lett. 84, 125–128.
- Dobrosotskaya, I.Y., Seegmiller, A.C., Brown, M.S., Goldstein, J.L., Rawson, R.B., 2002. Regulation of SREBP processing and membrane lipid production by phospholipids in *Drosophila*. Science (80-.) 296, 879–883. <https://doi.org/10.1126/science.1071124>.
- Driessnack, M.K., Jamwal, A., Niyogi, S., 2017a. Effects of chronic exposure to waterborne copper and nickel in binary mixture on tissue-specific metal accumulation and reproduction in fathead minnow (*Pimephales promelas*). Chemosphere 185, 964–974. <https://doi.org/10.1016/j.chemosphere.2017.07.100>.
- Driessnack, M.K., Jamwal, A., Niyogi, S., 2017b. Effects of chronic waterborne cadmium and zinc interactions on tissue-specific metal accumulation and reproduction in fathead minnow (*Pimephales promelas*). Ecotoxicol. Environ. Saf. 140, 65–75. <https://doi.org/10.1016/j.ecoenv.2017.02.023>.
- Felton, G.W., Summers, C.B., 1995. Antioxidant systems in insects. Arch. Insect Biochem. Physiol. 29, 187–197. <https://doi.org/10.1002/arch.940290208>.
- Floury, M., Usseglio-Polatera, P., Ferreol, M., Delattre, C., Souchon, Y., 2013. Global climate change in large European rivers: long-term effects on macro-invertebrate communities and potential local confounding factors. Glob. Chang. Biol. 19, 1085–1099. <https://doi.org/10.1111/gcb.12124>.
- Folch, J., Lees, M., Sloane Stanley, G.H., 1957. A simple method for the isolation and purification of total lipides from animal tissues. J. Biol. Chem. 226, 497–509.
- García, J.J., Martínez-Ballarín, E., Millán-Plano, S., Allué, J.L., Albendea, C., Fuentes, L., Escanero, J.F., 2005. Effects of trace elements on membrane fluidity. J. Trace Elem. Med. Biol. 19, 19–22. <https://doi.org/10.1016/j.jtemb.2005.07.007>.
- Georgieva, T., Dunkov, B.C., Harizanova, N., Ralchev, K., Law, J.H., 1999. Iron availability dramatically alters the distribution of ferritin subunit messages in *Drosophila melanogaster*. Proc. Natl. Acad. Sci. U.S.A. 96, 2716–2721.
- Gilbert, L.I., O'Connor, J.D., 2012. Lipid metabolism and transport in arthropods. In: Florkin, M. (Ed.), Chemical Zoology V5. Academic Press, pp. 229–253.
- Gilbert, L.I., Rybczynski, R., Warren, J.T., 2002. Control and biochemical nature of the ecdysteroidogenic pathway. Annu. Rev. Entomol. 47, 883–916. <https://doi.org/10.1146/annurev.ento.47.091201.145302>.
- Gross, M.Y., Maycock, D.S., Thorndyke, M.C., Morrirt, D., Crane, M., 2001. Abnormalities in sexual development of the amphipod *Gammarus pulex* (L.) found below sewage treatment works. Environ. Toxicol. Chem. 20, 1792–1797.
- Ha, M.-H., Choi, J., 2008. Effects of environmental contaminants on hemoglobin of larvae of aquatic midge, *Chironomus riparius* (Diptera: chironomidae): a potential biomarker for ecotoxicity monitoring. Chemosphere 71, 1928–1936. <https://doi.org/10.1016/j.chemosphere.2008.01.018>.
- Henrich, V.C., Rybczynski, R., Gilbert, L.I., 1999. Peptide hormones, steroid hormones, and puffs: mechanisms and models in insect development. Vitam. Horm. 55, 73–125.
- Herrero, Ó., Aquilino, M., Sánchez-Argüello, P., Planelló, R., 2018. The BPA-substitute bisphenol S alters the transcription of genes related to endocrine, stress response and biotransformation pathways in the aquatic midge *Chironomus riparius* (Diptera, Chironomidae). PLoS One 13, e0193387. <https://doi.org/10.1371/journal.pone.0193387>.
- Herrero, Ó., Morcillo, G., Planelló, R., 2017. Transcriptional deregulation of genetic biomarkers in *Chironomus riparius* larvae exposed to ecologically relevant concentrations of di(2-ethylhexyl) phthalate (DEHP). PLoS One 12, e0171719. <https://doi.org/10.1371/journal.pone.0171719>.
- Herrero, Ó., Planelló, R., Morcillo, G., 2016. The ribosome biogenesis pathway as an early target of benzyl butyl phthalate (BBP) toxicity in *Chironomus riparius* larvae. Chemosphere 144, 1874–1884. <https://doi.org/10.1016/j.chemosphere.2015.10.051>.
- Ilkova, J., Michailova, P., Szarek-Gwiazda, E., Kownacki, A., Ciszewski, D., 2018. *Prodiamesa olivacea* Meigen and *Prodiamesa bureshi* Michailova (Diptera, Chironomidae, Prodiamesinae) as a candidate for assessing the genotoxicity of trace metals in fluvial sediments. Environ. Monit. Assess. 190, 542. <https://doi.org/10.1007/s10661-018-6928-4>.
- Im, J., Chatterjee, N., Choi, J., 2019. Genetic, epigenetic, and developmental toxicity of *Chironomus riparius* raised in metal-contaminated field sediments: a multi-generational study with arsenic as a second challenge. Sci. Total Environ. 672, 789–797. <https://doi.org/10.1016/j.scitotenv.2019.04.013>.
- Jordão, R., Casas, J., Fabrias, G., Campos, B., Piña, B., Lemos, M.F.L., Soares, A.M.V.M., Tauler, R., Barata, C., 2015. Obesogens beyond vertebrates: lipid perturbation by tributyltin in the Crustacean *Daphnia magna*. Environ. Health Perspect. 123, 813–819. <https://doi.org/10.1289/ehp.1409163>.
- Klingenberg, C.P., 2011. MorphoJ: an integrated software package for geometric morphometrics. Mol. Ecol. Resour. 11, 353–357. <https://doi.org/10.1111/j.1755-0998.2010.02924.x>.
- Kühnlein, R.P., 2012. Thematic review series: lipid droplet synthesis and metabolism: from yeast to man. Lipid droplet-based storage fat metabolism in *Drosophila*. J. Lipid Res. 53, 1430–1436. <https://doi.org/10.1194/jlr.R024299>.
- Langer-Jaeschrich, M., Köhler, H.-R., Gerhardt, A., 2010. Assessing toxicity of the insecticide thiacloprid on *Chironomus riparius* (insecta: Diptera) using multiple end points. Arch. Environ. Contam. Toxicol. 58, 963–972. <https://doi.org/10.1007/s00244-009-9420-x>.
- Lee, S.-M., Lee, S.-B., Park, C.-H., Choi, J., 2006. Expression of heat shock protein and hemoglobin genes in *Chironomus tentans* (Diptera, chironomidae) larvae exposed to various environmental pollutants: a potential biomarker of freshwater monitoring. Chemosphere 65, 1074–1081. <https://doi.org/10.1016/j.chemosphere.2006.02.042>.
- Lee, S.-W., Chatterjee, N., Im, J.-E., Yoon, D., Kim, S., Choi, J., 2018. Integrated approach of eco-epigenetics and eco-metabolomics on the stress response of bisphenol-A exposure in the aquatic midge *Chironomus riparius*. Ecotoxicol. Environ. Saf. 163, 111–116. <https://doi.org/10.1016/j.ecoenv.2018.06.084>.
- Lin, X., Smagghe, G., 2018. Roles of the insulin signaling pathway in insect development and organ growth. Peptides. <https://doi.org/10.1016/j.peptides.2018.02.001>.
- Long, S.M., Tull, D.L., Jeppe, K.J., De Souza, D.P., Dayalan, S., Pettigrove, V.J., McConville, M.J., Hoffmann, A.A., 2015. A multi-platform metabolomics approach demonstrates changes in energy metabolism and the transsulfuration pathway in *Chironomus tepperi* following exposure to zinc. Aquat. Toxicol. 162, 54–65. <https://doi.org/10.1016/j.aquatox.2015.03.009>.
- MacDonald, D.D., Ingersoll, C.G., Berger, T.A., 2000. Development and evaluation of consensus-based sediment quality Guidelines for freshwater ecosystems. Arch. Environ. Contam. Toxicol. 39, 20–31. <https://doi.org/10.1007/s002440010075>.
- Mamon, M.A.C., Añano, J.A.P., Abanador, L.C., Agcaoili, G.J.T., Sagum, C.B., Pagliawan, R.L.H., Tapere, J.M.B., Agravante, J.B.M., Arevalo, J.H.G., Minalang, A.J.A., 2016. Pollutant exposure in manila bay: effects on the allometry and histological structures of *Perna viridis* (linn.). Asian Pacific J. Reprod. 5, 240–246. <https://doi.org/10.1016/j.apjr.2016.03.002>.
- Martínez-Paz, P., 2018. Response of detoxification system genes on *Chironomus riparius* aquatic larvae after antibacterial agent triclosan exposures. Sci. Total Environ. 624, 1–8. <https://doi.org/10.1016/j.scitotenv.2017.12.107>.
- Martínez, E.A., Moore, B.C., Schaumloffel, J., Dasgupta, N., 2003. Morphological abnormalities in *Chironomus tentans* exposed to cadmium-and copper-spiked sediments. Ecotoxicol. Environ. Saf. 55, 204–212.
- Maynard, J.C., Pham, T., Zheng, T., Jockheck-Clark, A., Rankin, H.B., Newgard, C.B., Spana, E.P., Nicchitta, C.V., 2010. Gp93, the *Drosophila* GRP94 ortholog, is required for gut epithelial homeostasis and nutrient assimilation-coupled growth control. Dev. Biol. 339, 295–306. <https://doi.org/10.1016/j.ydbio.2009.12.023>.
- Méndez-Fernández, L., 2013. Metal Toxicity and Bioaccumulation in Tubifex Tubifex (Müller) (Annelida) Exposed to River Sediments from Northern Spain. Thesis Dissertation. University of Basque Country (UPV/EHU), Bilbao, Spain.
- Méndez-Fernández, L., Martínez-Madrid, M., Rodríguez, P., 2013. Toxicity and Critical Body Residues of Cd, Cu and Cr in the aquatic oligochaete *Tubifex tubifex* (Müller) based on lethal and sublethal effects. Ecotoxicology 22, 1445–1460.
- Miller, M.P., Hendricks, A.C., 1996. Zinc resistance in *Chironomus riparius*: evidence for physiological and genetic components. J. North Am. Benthol. Soc. 15, 106–116. <https://doi.org/10.2307/1467436>.
- Missirlis, F., Kosmidis, S., Brody, T., Mavrakis, M., Holmberg, S., Odenwald, W.F., Skoulakis, E.M.C., Rouault, T.A., 2007. Homeostatic mechanisms for iron storage revealed by genetic manipulations and live imaging of *Drosophila* ferritin. Genetics 177, 89–100. <https://doi.org/10.1534/genetics.107.075150>.
- Moncaleano-Niño, A.M., Barrios-Latorre, S.A., Poloche-Hernández, J.F., Becquet, V., Huet, V., Villamil, L., Thomas-Guyon, H., Ahrens, M.J., Luna-Acosta, A., 2017. Alterations of tissue metallothionein and vitellogenin concentrations in tropical cup oysters (*Saccostrea* sp.) following short-term (96 h) exposure to cadmium. Aquat. Toxicol. 185, 160–170. <https://doi.org/10.1016/j.aquatox.2017.02.011>.
- Murphy, M.E., 2013. The HSP70 family and cancer. Carcinogenesis 34, 1181–1188. <https://doi.org/10.1093/carcin/bgt111>.
- Nair, P.M.G., Park, S.Y., Choi, J., 2013. Characterization and expression of cytochrome p450 cDNA (CYP9AT2) in *Chironomus riparius* fourth instar larvae exposed to multiple xenobiotics. Environ. Toxicol. Pharmacol. 36, 1133–1140. <https://doi.org/10.1016/j.etap.2013.08.011>.
- Nair, P.M.G., Park, S.Y., Choi, J., 2011. Expression of catalase and glutathione S-transferase genes in *Chironomus riparius* on exposure to cadmium and

- nonylphenol. *Comp. Biochem. Physiol. C Toxicol. Pharmacol.* 154, 399–408. <https://doi.org/10.1016/j.cbpc.2011.07.008>.
- Nikolić, T.V., Kojić, D., Orčić, S., Batinić, D., Vukašinić, E., Blagojević, D.P., Purać, J., 2016. The impact of sublethal concentrations of Cu, Pb and Cd on honey bee redox status, superoxide dismutase and catalase in laboratory conditions. *Chemosphere* 164, 98–105. <https://doi.org/10.1016/j.chemosphere.2016.08.077>.
- OECD, 2011. Test No. 235: Chironomus sp., Acute Immobilisation Test. Organisation for Economic Co-operation and Development, Paris.
- OECD, 2010. Test No. 233: Sediment-Water Chironomid Life-Cycle Toxicity Test Using Spiked Water or Spiked Sediment. Organisation for Economic Co-operation and Development, Paris.
- OECD, 2004a. Test No. 218: Sediment-Water Chironomid Toxicity Test Using Spiked Sediment. Organisation for Economic Co-operation and Development, Paris.
- OECD, 2004b. Test No. 219: Sediment-Water Chironomid Toxicity Test Using Spiked Water. Organisation for Economic Co-operation and Development, Paris.
- Olakkaran, S., Antony, A., Kizhakke Purayil, A., Tilagul Kumbhar, S., Hunasanahally Puttaswamygowda, G., 2018. Lead modulated Heme synthesis inducing oxidative stress mediated Genotoxicity in *Drosophila melanogaster*. *Sci. Total Environ.* 634, 628–639. <https://doi.org/10.1016/j.scitotenv.2018.04.004>.
- Olmstead, A.W., LeBlanc, G.A., 2000. Effects of endocrine-active chemicals on the development of sex characteristics of *Daphnia magna*. *Environ. Toxicol. Chem.* 19, 2107–2113. <https://doi.org/10.1002/etc.5620190821>.
- Osmulski, P., Leyko, W., 1986. Structure, function and physiological role of chironomus haemoglobin. *Comp. Biochem. Physiol. Part B Comp. Biochem.* 85, 701–722. [https://doi.org/10.1016/0305-0491\(86\)90166-5](https://doi.org/10.1016/0305-0491(86)90166-5).
- Palmer, A., Strobeck, C., 2003. Fluctuating asymmetry analyses revisited. In: Polak, M. (Ed.), *Developmental Instability: Causes and Consequences*. Oxford University Press, New York, pp. 279–319.
- Park, K., Park, J., Kim, J., Kwak, I.-S., 2010. Biological and molecular responses of Chironomus riparius (Diptera, Chironomidae) to herbicide 2,4-D (2,4-dichlorophenoxyacetic acid). *Comp. Biochem. Physiol. C Toxicol. Pharmacol.* 151, 439–446. <https://doi.org/10.1016/j.cbpc.2010.01.009>.
- Pesquera, A., Velasco, F., 1989. The arditurri Pb-Zn-F-Ba deposit (Cinco Villas massif, Basque Pyrenees): a deformed and metamorphosed stratiform deposit. *Miner. Depos.* 24, 199–209. <https://doi.org/10.1007/BF00206443>.
- Pham, D.Q.D., Winzerling, J.J., 2010. Insect ferritins: typical or atypical? *Biochim. Biophys. Acta Gen. Subj.* 1800, 824–833. <https://doi.org/10.1016/j.bbagen.2010.03.004>.
- Planelló, R., Martínez-Guitarte, J.L., Morcillo, G., 2008. The endocrine disruptor bisphenol A increases the expression of HSP70 and ecdysone receptor genes in the aquatic larvae of *Chironomus riparius*. *Chemosphere* 71, 1870–1876. <https://doi.org/10.1016/j.chemosphere.2008.01.033>.
- Planelló, R., Martínez-Guitarte, J.L., Morcillo, G., 2010. Effect of acute exposure to cadmium on the expression of heat-shock and hormone-nuclear receptor genes in the aquatic midge *Chironomus riparius*. *Sci. Total Environ.* 408, 1598–1603. <https://doi.org/10.1016/j.scitotenv.2010.01.004>.
- Planelló, R., Servia, M.J., Gómez-Sande, P., Herrero, Ó., Cobo, F., Morcillo, G., 2015. Transcriptional responses, metabolic activity and mouthpart deformities in natural populations of *Chironomus riparius* larvae exposed to environmental pollutants. *Environ. Toxicol.* 30, 383–395. <https://doi.org/10.1002/tox.21893>.
- R Core Team, 2018. R: A Language and Environment for Statistical Computing. R Foundation for Statistical Computing, Vienna, Austria.
- Reynoldson, T.B., Day, K.E., Clarke, C., Milani, D., 1994. Effect of indigenous animals on chronic end points in freshwater sediment toxicity tests. *Environ. Toxicol. Chem.* 13, 973–977. <https://doi.org/10.1002/etc.5620130616>.
- Roy, S.G., Hansen, I.A., Raikhel, A.S., 2007. Effect of insulin and 20-hydroxyecdysone in the fat body of the yellow fever mosquito, *Aedes aegypti*. *Insect Biochem. Mol. Biol.* 37, 1317–1326. <https://doi.org/10.1016/j.ibmb.2007.08.004>.
- Salin, K., Auer, S.K., Rey, B., Selman, C., Metcalfe, N.B., 2015. Variation in the link between oxygen consumption and ATP production, and its relevance for animal performance. *Proceedings. Biol. Sci.* 282, 20151028. <https://doi.org/10.1098/rspb.2015.1028>.
- Scheitz, C.J.F., Guo, Y., Early, A.M., Harshman, L.G., Clark, A.G., 2013. Heritability and inter-population differences in lipid profiles of *Drosophila melanogaster*. *PLoS One* 8, e72726. <https://doi.org/10.1371/journal.pone.0072726>.
- Su, H., Yang, Y., Qian, Y., Ye, Z., Chen, Y., Yang, Y., 2019. Effects of lead stress on Vg expression in the beet armyworm over five successive generations. *J. Integr. Agric.* 18, 134–142. [https://doi.org/10.1016/S2095-3119\(18\)61931-8](https://doi.org/10.1016/S2095-3119(18)61931-8).
- Swevers, L., Iatrou, K., 2009. Ecdysteroids and ecdysteroid signaling pathways during insect oogenesis. In: Smagghe, G. (Ed.), *Ecdysone: Structures and Functions*. Springer Netherlands, Dordrecht, pp. 127–164.
- Tocanne, J.F., Teissié, J., 1990. Ionization of phospholipids and phospholipid-supported interfacial lateral diffusion of protons in membrane model systems. *Biochim. Biophys. Acta* 1031, 111–142.
- Urteaga, M., 2008. El vasconum saltus y oiasso. *Boletín Arkeolan* 15, 173–188.
- USEPA, 2007. Method 3051A (SW-846): Microwave Assisted Acid Digestion of Sediments, Sludges, and Oils. United States Environmental Protection Agency, Washington, DC, USA.
- Vandesompele, J., De Preter, K., Pattyn, F., Poppe, B., Van Roy, N., De Paepe, A., Speleman, F., 2002. Accurate normalization of real-time quantitative RT-PCR data by geometric averaging of multiple internal control genes. *Genome Biol.* 3 <https://doi.org/10.1186/gb-2002-3-7-research0034> research0034.1.
- Vörösmarty, C.J., Green, P., Salisbury, J., Lammers, R.B., 2000. Global water resources: vulnerability from climate change and population growth. *Science* 289, 284–288.
- Weis, J.S., 2014. Larval development. In: *Physiological, Developmental and Behavioral Effects of Marine Pollution*. Springer Netherlands, Dordrecht, pp. 215–251.
- Wheelock, C.E., Eder, K.J., Werner, L., Huang, H., Jones, P.D., Brammell, B.F., Elskus, A.A., Hammock, B.D., 2005. Individual variability in esterase activity and CYP1A levels in Chinook salmon (*Oncorhynchus tshawytscha*) exposed to esfenvalerate and chlorpyrifos. *Aquat. Toxicol.* 74, 172–192. <https://doi.org/10.1016/j.aquatox.2005.05.009>.
- Yang, J., Liu, D., Dahms, H.-U., Wang, L., 2015. Cadmium inhibits the vitellogenesis of freshwater crab *Sinopotamon henanense*. *Environ. Toxicol. Chem.* 34, 1609–1616. <https://doi.org/10.1002/etc.2958>.
- Yepiskoposyan, H., Egli, D., Fergestad, T., Selvaraj, A., Treiber, C., Multhaup, G., Georgiev, O., Schaffner, W., 2006. Transcriptome response to heavy metal stress in *Drosophila* reveals a new zinc transporter that confers resistance to zinc. *Nucleic Acids Res.* 34, 4866–4877.
- Zhao, J., Sun, Y., Xiao, L., Tan, Y., Bai, L., 2016. Molecular characterization and expression of vitellogenin gene from *Spodoptera exigua* exposed to cadmium stress. *Gene* 593, 179–184. <https://doi.org/10.1016/j.gene.2016.08.025>.